JLB

Article

TLR-activated conventional DCs promote γ-secretase-mediated conditioning of plasmacytoid DCs

Begoña Pérez-Cabezas, Mar Naranjo-Gómez,* Marta Ruiz-Riol,* Patricia Bastos-Amador,* Marco A. Fernández,† Francesc Carmona,‡ Fatima Nuñez,§ Ricardo Pujol-Borrell,* and Francesc E. Borràs*,1*

*Laboratori d'Immunobiologia i Diagnòstic Molecular (LIRAD), Banc de Sang i Teixits (BST), Departament de Biologia Cel·lular, Fisiologia i Immunologia, Universitat Autònoma de Barcelona, Institut d'Investigació Germans Trias i Pujol, and †Unitat de citometria, Institut d'investigació Germans Trias i Pujol, Badalona, Barcelona, Spain; ‡Department d'estadística, Universitat de Barcelona, Barcelona, Spain; and §Unitat científico-tècnica de suport, Institut d'Investigació Vall d'Hebron, Barcelona, Spain

RECEIVED SEPTEMBER 6, 2011; REVISED APRIL 3, 2012; ACCEPTED APRIL 6, 2012. DOI: 10.1189/jlb.0911452

ABSTRACT

Cooperative events between DC subsets involve cell contact and soluble factors. Upon viral challenge, murine pDCs induce cDC cooperation through CD40-CD40L interactions and IL-15 secretion, whereas in humans, the same effect is mediated by IFN-α. Conversely, during bacterial infections, pDC maturation may be induced by activated cDCs, although no mechanisms had been described so far. Here, we investigate how human pDCs are "conditioned" by cDCs. Blood-borne DC subsets (cDCs and pDCs) were sorted from healthy donors. IL-3-maintained pDCs were cocultured with LPS-activated, poly (I:C)-activated, or control cDCs [cDC_{LPS}, $cDC_{P(I:C)}$, cDC_{CTRL}]. Coculture experiments showed that cDC_{LPS}-conditioned pDCs up-regulated maturation markers, such as CD25 and CD86, whereas SNs contained higher amounts of IL-6 and CCL19 compared with control conditions. Gene-expression analyses on sorted cDC_{LPS} or $cDC_{P(I:C)}$ conditioned pDCs confirmed the induction of several genes, including IL-6 and CCL19 and remarkably, several Notch target genes. Further studies using the γ-secretase/Notch inhibitor DAPT and soluble Notch ligands resulted in a significantly reduced expression of canonical Notch target genes in conditioned pDCs. DAPT treatment also hampered the secretion of CCL19 (but not of IL-6) by cDC_{LPS} conditioned pDCs. These results reveal the involvement of γ-secretase-mediated mechanisms, including the Notch pathway, in the cell contact-dependent communication between human DC subsets. The resulting partial activation of pDCs after encountering with mature cDCs endows pDCs with an accessory function that may contribute to T cell recruitment and activation. *J. Leukoc. Biol.* 92: 133–143; 2012.

Introduction

DCs play an essential role in immune homeostasis. Blood DCs in humans comprise two well-characterized blood DC populations—cDC and pDC [1–3]. These populations exhibit multiple differences between them, regarding morphology, phenotype, TLR expression, as well as cytokine and chemokine secretion [4, 5]. Furthermore, other potential differences still under debate between DC subsets refer to their diverse homing profile and their different capacity for antigen capture. cDCs are particularly efficient on antigen presentation, as a result of their high endocytic activity, their ability to retain long-lived MHC-II peptide complexes on the cellular membrane, and their capacity to cross-present antigens [6]. In contrast, pDCs are excellent responders to viral stimulation (i.e., secreting IFN-α) but far less competent compared with cDCs on antigen uptake and presentation [6–10]. These rather exclusive features prompted several groups to study the possible coordination between DC subsets to promote an efficient immune response.

In the context of the immune response, it is conceived that the DC type receiving the danger signal will initiate a cell-contact interaction between DC subsets. This contact may take place in the LNs or in the inflamed tissues, where DCs are re-

Abbreviations: AITD=autoimmune thyroid disease, AITG=autoimmune thyroid gland, BATF=basic leucine zipper transcription factor, ATF-like, BDCA=blood DC antigen, BST=Banc de Sang i Teixits, CD2L/CD40L=CD2/CD40 ligand, cDC=conventional DC, Ct=comparative threshold, CTRL=control, DAPT=N-[N-(3,5-difluorophenacetyl)-L-alanyl]-S-phenylglycine t-butyl ester, DE=differentially expressed, HES1=hairy/enhancer of split 1, HEY1=hairy/enhancer-of-split related with YRPW motif 1, HUGTIP=Hospital Universitari Germans Trias i Pujol, Jag=jagged, pDC=plasmacytoid DC, poly (I:C)/P(I:C)=polyinosinic:polycytidylic acid, R848=resiquimod, rh=recombinant human, s=soluble, SN=supernatant

The online version of this paper, found at www.jleukbio.org, includes supplemental information.

1. Correspondence: LIRAD-BST, Germans Trias i Pujol Research Institute, Crtra. del Canyet s/n, edifici Escoles, 08916, Badalona, Barcelona, Spain. E-mail: feborras@igtp.cat

cruited during the course of an inflammatory response. In this sense, a physical association between human pDCs and cDCs has been reported in the skin of cutaneous lupus erythematosus patients [11] and in the spleen of HIV-infected individuals [12]. Functionally, coculturing human pDCs with cDCs increases alloantigen presentation, as revealed by a higher level of alloproliferation and of IFN-γ production by T cells [13, 14]. In mice, pDCs improve cDC activation and CTL generation via CD40-CD40L interaction [15] and through IL-15 secretion [16] but not IFN-α [17]. In contrast, conditioning of human cDCs by activated pDCs (after virus or CpG DNA exposure) is IFN-α-dependent [18–20]. Conversely, coculture of pDCs with bacterially activated cDCs induces pDC phenotype maturation [14], suggesting a possible role for pDCs as accessory cells during bacterial infections. In contrast to that observed in mice, this induced maturation requires cell contact but is not dependent on CD40-CD40L interaction.

In this study, we aimed to deepen in the effects and mechanisms of human DC coordination. We first confirmed that DC subsets are in close contact in LNs and also in infiltrated AITG, thus providing the physiological environment for cell contact-dependent events. Second, we demonstrated that TLR-activated cDCs directed phenotype maturation, secretion of IL-6 and CCL19, and differential gene expression in conditioned pDCs. Finally, the identification of Notch target genes among those up-regulated on conditioned pDCs delineated the involvement of γ-secretase-mediated mechanisms, including the Notch signaling pathway, in the functional activation of pDCs by TLR-activated cDCs.

MATERIALS AND METHODS

Culture media and reagents

As culture media, we used RPMI 1640 (Gibco, Invitrogen, Carlsbad, CA, USA), supplemented with 10% heat-inactivated FBS (Gibco, Invitrogen), 2 mM L-glutamine (Sigma-Aldrich, St. Louis, MO, USA), 100 U/mL penicillin (Cepa S.L, Madrid, Spain), and 100 μg/mL streptomycin (Laboratorios Normon S.A, Madrid, Spain). rhIL-3 (R&D Systems, Minneapolis, MN, USA) was added at 10 ng/mL to all cultures, where pDCs were present. R848 (Alexis Biochemicals, San Diego, CA, USA), LPS (Sigma-Aldrich), and poly (I:C) (Sigma-Aldrich) were used at 5 μM, 1 μg/mL, and 10 μg/mL, respectively, at the indicated times. In some cases, the γ-secretase inhibitor IX DAPT (Calbiochem, Merck KGaA, Darmstadt, Germany) was present throughout the entire culture at 10 μM. This reagent was tested for the absence of endotoxin using the multi-test Limulus amoebocyte lysate Pyrogent Plus (Lonza Group, Switzerland) with a sensitivity of 0.05 ng/mL. DAPT, considered the most chemically selective inhibitor of the Notch pathway [21], prevents the release and translocation to the nucleus of the intracellular Notch domain, inhibiting the downstream Notch pathway. srhJag1 Fc chimera (R&D Systems) was used in some competition experiments at a concentration of 10 μg/mL in 0.5% FBS containing RPMI.

mAb

The following murine mAb were used: purified BDCA-2 (Miltenyi Biotec, GmbH, Bergisch Gladbach, Germany) and CD11c (Biosource International, Carlsbad, CA, USA); FITC-labeled mAb, including CD45 RA, CD86 (BD Biosciences, San Jose, CA, USA); CD4, CD16 (ImmunoTools, Germany); and CD123, BDCA-2 (Miltenyi Biotec). PE-labeled mAb were CD3, CD25, CD40, CD83, CD86, and CD123 (BD Biosciences); CD14 (ImmunoTools); and BDCA-1, BDCA-2 (Miltenyi Biotec). Also, PE-Cy5-labeled CD11c (BD Biosciences), allophycocyanin-labeled CD83 (BD Biosciences), and allophycocyanin-Cy7-labeled HLA-DR (BD Biosciences) mAb were used; isotype-matched antibodies were used as controls.

Immunostaining and flow cytometry

Cells were washed, resuspended in 50 μl PBS, and incubated with mAb for 20 min at 4°C. Acquisition was performed in a FACSCanto II flow cytometer using the Standard FACSDiva software (BD Biosciences). Subsequent analyses were performed using FlowJo software 7 (Tree Star, Ashland, OR, USA). Samples were gated using forward- and side-scatter to exclude dead cells and debris.

Patients and samples

LN samples and thyroid tissue were obtained from the Histopathology Department of the HUGTIP. Patient informed consent was obtained, and protocols were approved by the ethical committee of the HUGTIP. Immediately after surgery, samples were snap-frozen in isopentane and stored at −70°C until immunofluorescence staining. LN samples (n=3) were obtained from patients suffering lymphoma, in which ganglionic cords were removed. The second LN of each ganglionic cord, showing no histological evidence of tumor, was considered "healthy", removed, and used in this study. AITG were obtained from patients diagnosed with AITDs (n=6) attended at the Endocrinology Unit at the HUGTIP or at Hospital Universitari Vall d'Hebron. All clinical data and the histological study of these samples have been published earlier [22].

Immunofluorescence staining of tissue sections

Tissue cryosections (4 μm) were stained by the indirect immunofluorescence technique, as described before [23]. pDCs and cDCs were detected using anti-BDCA-2 (Miltenyi Biotec) and anti-CD11c (Biosource International), respectively. Isotype-specific serum conjugates, goat anti-mouse IgG_1 labeled with Alexa 488 (Molecular Probes, Invitrogen, Carlsbad, CA, USA), and goat anti-mouse IgG_{2a} labeled with Rhodamine (TRITC; Southern Biotech, Birmingham, AL, USA) were used. These secondary antibodies were diluted in PBS containing 1% FBS. The controls included nonimmune sera, unrelated mAb as primary antibody, and omission of each of the layers. Sections were examined under a UV fluorescent microscope (Axioskop II, Zeiss, Oberkochen, Germany). Images were acquired using a high-sensitivity video camera (Hamamatsu, Hamamatsu City, Japan) and the Openlab 2 software (Improvision, Coventry, UK).

DC isolation

Buffy coats, provided by the BST, were obtained from healthy blood donors with their concern and following the Institutional Standard Operating Procedures for blood donation and processing. Samples were processed as described before [13]. Briefly, PBMCs were isolated by Ficoll-Paque density gradient centrifugation (400 g, 25 min; Lymphoprep, AxisShield, Oslo, Norway), and $CD3^+$ cells were depleted by RosetteSep human CD3 depletion cocktail (Stemcell Technologies, Tukwila, WA, USA). Recovered cells were washed twice in PBS and counted using Perfect Count microspheres (Cytognos S.L, Salamanca, Spain). Monocytes were depleted by positive selection using human CD14 MicroBeads and autoMACS columns (Miltenyi Biotec). The remaining population was incubated with FITC-CD4, PE-CD14, PE-CD3, and PE-Cy5-CD11c mAb and sorted in a FACSAria II cell sorter (BD Biosciences). PE-positive cells were discarded. Double-positive cells for CD4 and CD11c were sorted as cDCs, whereas single-positive CD4 cells were sorted as pDCs. In all samples, purity was over 99% (Supplemental Fig. 1A). Whereas pDCs showed a unique population defined by CD123 and BDCA-2 expression (Supplemental Fig. 1B), cDCs included two major subsets ($CD16^+CD123^+CD14^{low}BDCA1^-$ and $CD16^-CD123^{low}CD14^{low/-}BDCA1^+$; Supplemental Fig. 1C), as described before [2]. Viability (>90%) of sorted populations was assessed by Annexin V+ 7-amino-actinomycin D labeling (BD Biosciences). Immaturity of isolated cells was revealed by the low/negative expression of CD40, CD83, and CD86.

pDC and cDC cocultures

Sorted pDCs and cDCs were cultured separately for 16 h in 96-well, round-bottom plates at 5×10^4 cells/well (Nunc, Roskilde, Denmark). During this time, pDCs were maintained with IL-3 (10 ng/mL), whereas cDCs were cultured in resting conditions (cDC_{CTRL}) or under activation by LPS (1 μg/mL; cDC_{LPS}) or poly (I:C) [10 μg/mL; $cDC_{P(I:C)}$]. Before coculturing, cells were washed extensively to remove dead cells and soluble factors. After that, pDCs were cocultured with cDC_{CTRL} or cDC_{LPS} at a ratio of 1:1 during 24 h (for phenotype analysis and SN determinations) or with cDC_{CTRL}, cDC_{LPS}, and in some experiments, with $cDC_{P(I:C)}$ during 5 h (for gene expression experiments) in the presence of IL-3 (10 ng/mL). DAPT (5 μM) and srhJag1 (10 μg/mL) were also added to the cocultures when indicated. For RNA studies, pDCs were CFSE-labeled before coculturing, as described previously [13]. Then, pDCs and cDCs were sorted again as $CFSE^+CD11c^-$/$CFSE^-CD11c^+$ cells, respectively. Purity of pDCs was consistently 100%, as confirmed by CD123 and BDCA-2 staining. Additional controls used were isolated pDCs cultured in the presence of IL-3 or IL-3 + LPS (1 μg/mL) or IL-3 + R848 (5 μM) for 5 h or 24 h.

Measurement of cytokine and chemokine production

IL-6, TNF-α, IFN-α, CCL1, CXCL9, CXCL10, CXCL11, and CCL19 were determined on cDC/pDC coculture SNs using the Milliplex Multi-Analyte Profiling (Millipore, Bedford, MA, USA), following the overnight protocol described by the manufacturer. In these experiments, cDCs were stimulated as described previously. After stimulation, cDCs were washed extensively and cultured alone or cocultured with pDCs. These SNs were collected after 24 h and analyzed for the presence of the mentioned proteins. In the indicated experiments, DAPT was added to the cultures to study the implication of the Notch pathway in cytokine regulation. The minimum detectable concentration (pg/mL) of each protein was 0.3 for IL-6, 0.1 for TNF-α, 24.5 for IFN-α, 0.5 for CCL1, 10.3 for CXCL9, 1.2 for CXCL10, 0.4 for CXCL11, and 2.1 for CCL19. All cytokines measured were over the detection limit.

Cell migration assays

pDCs, cDC_{CTRL}, and cDC_{LPS} were cultured alone or in combination at a concentration of 1×10^6 cells/700 μl RPMI + 0.5% FBS during 24 h. Then, 250 μl coculture SNs (pDC+cDC_{CTRL} or pDC+cDC_{LPS}) or a mixture of 125 μl pDC SNs + 125 μl cDC SNs (SN pDC+SN cDC_{CTRL} or SN pDC+SN cDC_{LPS}) were placed in the lower chamber of 96-well Corningstar plates (3 μm membrane pore size, Corning B.V. Life Sciences, Amsterdam, The Netherlands). Where mentioned, 10 μg/mL blocking antibody for CCL19 (R&D Systems) or human IgGs were added to the SNs, 30 min before the beginning of the experiment. Autologous PBMCs (150×10^3) were added to the upper chamber, and plates were incubated for 4 h at 37°C with 5% CO_2. Cells migrating to the lower chamber were collected (50 μl) and counted using Perfect Count microspheres (Cytognos S.L).

RNA isolation, labeling, and hybridization

RNA was extracted from sorted pDCs using the Qiagen RNeasy Micro Kit (Qiagen, Hilden, Germany). Quality, purity, and concentration were assessed using the Bioanalyzer 2100 (Agilent Technologies, Santa Clara, CA, USA). RNA integrity was greater than seven in all samples included in the assay. Total extracted RNA was used to synthesize ds-cDNA with the Two Cycle cDNA Synthesis Kit (Affymetrix, Santa Clara, CA, USA). Biotin-labeled antisense cRNA was obtained using the same kit starting with 5 ng total RNAs and the oligo dT primer, 5′GGCCAGTGAATTGTAATACGACTCACTATAGGGAGGCGG-$(dT)_{24}$. cRNAs were purified using the columns from the GeneChip Sample Cleanup Module (Affymetrix), and then 20 mg cRNAs was fragmented at 94°C for 30 min in 40 ml 40 mM Tris-acetate, pH 8.1, 100 mM KOAc, 30 mM $Mg(OAc)_2$. The fragmented samples were checked using the Bioanalyzer 2100 to verify their quality and then added to a hybridization cocktail containing control oligonucleotide B2 (50 pM) and eukaryotic hybridization controls (BioB, BioC, BioD, cre) at 1.5, 5, 25, and 100 pM final concentration, respectively, from the GeneChip Eukaryotic Hybridization Control Kit (Affymetrix), herring sperm DNA (0.1 mg/ml), and acetylated BSA (0.5 mg/ml). The Probe array used was the GeneChip Human Genome U133 Plus 2.0 Array, which covers >47,000 transcripts and represents ~39,000 human genes. The chip was prehybridized with 1× hybridization buffer [100 mM 2-(N-morpholino)ethanesulfonic acid, 1 M Na^+, 20 mM EDTA, 0.01% Tween 20] at 45°C for 10 min with rotation. The hybridization cocktail was heated to 99°C for 5 min, transferred to 45°C heat block for 5 min, and spun at maximum speed in a microfuge for 5 min. The hybridization mixture (200 mL) was used to fill the Affymetrix cartridge after removal of the hybridization buffer, and the arrays were hybridized at 45°C for 16 h with rotation in the Affymetrix GeneChip Hyb Oven 640. GeneChips were washed and marked with streptavidin PE in the Fluidics Station 450 (Affymetrix) using the protocol EukGE-WS2-v5 provided by Affymetrix. Once washed and streptavidin PE-marked, the GeneChips were scanned in an Agilent G3000 GeneArray scanner. Raw data are available at the ArrayExpress repository, European Bioinformatics Institute (http://www.ebi.ac.uk/microarray-as/ae/; provisional ID: E-MEXP-2555).

Microarray analysis

Images were processed using the Microarray Analysis Suite 5.0 (Affymetrix). All samples probed a high-quality cRNA (3′:5′ ratio of probe sets for GAPDH and β-actin of <1.5), and they were subsequently analyzed. Data were previously nonspecifically filtered to remove low-signal genes and low-variability genes. Then, DE genes between conditions were selected based on a linear model analysis with empirical Bayes moderation of the variance estimates following the methodology developed by Smyth [24]. Genes selected as being DE were clustered to look for common patterns of expression. Hierarchical clustering with euclidean distance was used to form the groups, and heat maps were used to visualize them. All statistical analyses were done in a linux-gnu machine (with Kubuntu 7.10 OS) using the free statistical language R 2.6.2 and the libraries developed for microarray data analysis by the Bioconductor Project (www.bioconductor.org). The main methods and tools used were described previously [25]. Genes showing a fold change $-1.5 \geq X \geq 1.5$, and $P \leq 0.05$ were considered further. Finally, heat maps were created using the heat map tool of the HIV database http://www.hiv.lanl.gov/.

Quantitative real-time RT-PCR

Total RNA from each sample was reverse-transcribed using the High-Capacity cDNA RT Kit (Applied Biosystems, Life Technologies, Carlsbad, CA, USA), as recommended by the manufacturer. cDNA obtained was preamplified with the TaqMan PreAmp Master Mix Kit (Applied Biosystems) for each gene-specific targets using a pool of TaqMan Gene Expression Assays as a source of primers. This preamplification reaction generated ~1,000- to 16,000-fold amplification of each gene-specific target without inducing any bias. The resulting preamplified material was diluted and used as the starting material for the subsequent singleplex real-time PCR with each of the following individual TaqMan Gene Expression Assays represented in the assay pool: CCL19, Hs00171149_m1; HES1, Hs00172878_m1; HEY1 Hs01114113_m1; IL-6, Hs00985641_m1; GAPDH, Hs99999905_m1. GAPDH mRNA levels were used as an endogenous control to normalize mRNA quantities. The relative mRNA levels of each gene were calculated as follows: relative mRNA expression = $2^{-(Ct\ gene - Ct\ GAPDH)}$ [26]. To minimize the effect of interindividual variability, the results were normalized to the internal control ($pDCs+cDCs_{CTRL}=1$).

Statistical analyses

Results are expressed as the mean ± SD unless otherwise stated. To minimize the effect of interindividual variability (inherent to human samples), in some experiments, the results are expressed as relative values to the control situation. Comparisons were conducted using the Wilcoxon signed-rank test for related but nonparametric observations. Analyses were per-

formed using the GraphPad Prism v4.00 software (GraphPad Software, La Jolla, CA, USA). A value of $P < 0.05$ was considered significant.

RESULTS

pDCs and cDCs are in close contact in LNs and autoimmune human tissue

Cell contact events are required for cooperation between DC subsets. Several studies have pointed out the physical association between human DC subsets in inflamed tissues [11, 12]. To further characterize this interaction in human tissues, noninflamed LNs were examined for the presence of both DC subsets. Close proximity and multiple cell contacts were observed between pDCs (BDCA-2+ cells) and cDCs (CD11c+ cells; **Fig. 1A**; $n=3$). A similar pattern was observed when thyroid glands from AITD patients were examined (Fig. 1B; $n=6$), in which infiltrating cDCs and pDCs were in close contact. These results further confirm that LNs and inflamed peripheral tissues are anatomical sites where cell contact events between DC subsets may occur under physiological and inflammatory conditions.

Cocultures of cDCs and pDCs induce quantitative changes on the IL-6 and CCL19 production

To explore the functional cooperation between human cDCs and pDCs, suggested by the cell contacts observed, in vitro coculture experiments were set up. Both DC subsets were obtained from the same donor and sorted to reach highly pure cDCs and pDCs (>99%). Upon isolation, pDCs were maintained overnight with IL-3, whereas cDCs were stimulated or not with LPS. Activated cDCs increased the expression of CD40, CD83, CD86, and HLA-DR and secreted CXCL9, CXCL11, CCL19, TNF-α, and IL-6 (data not shown). These activated and nonactivated cDCs were used as "conditioners" in coculture experiments with pDCs, as described in Materials and Methods.

After 24 h of coculture, cDC_{LPS} conditioned pDCs ($pDC+cDC_{LPS}$) showed a maturation profile, as revealed by the consistent increase in the levels of CD25, CD83, and CD86 compared with the control situation ($pDC+cDC_{CTRL}$; **Fig. 2A**). In control cultures, pDCs were maintained in control conditions (pDC+IL-3) or stimulated with the TLR7/TLR8 ligand R848 (pDC+R848), which promoted maximal activation. To further study the functional implications of pDC-cDC cooperation, we analyzed the secretion of several cytokines and chemokines in SNs from 24-h coculture experiments (Fig. 2B). Overall, coculture of pDC+cDC (especially $pDC+cDC_{LPS}$) revealed increased levels of CCL19 compared with pDCs or cDCs cultured alone. Further, IL-6 was increased in the coculturing conditions. The other cytokines and chemokines analyzed did not show any remarkable change. Finally, as it has been reported before [13, 14], $pDC+cDC_{LPS}$ exhibited an increased T cell allostimulatory capacity (data not shown).

CCL19 produced in $pDC+cDC_{LPS}$ cocultures induces cell migration

To ascertain whether the increased CCL19 detected in SNs from $pDC+cDC_{LPS}$ cocultures was functional, autologous PBMCs were used in migration experiments. In two different individuals, SNs from $pDC+cDC_{LPS}$ induced higher cell migration than SNs from $pDC+cDC_{CTRL}$ or a combination of SNs from pDCs+SNs from cDC_{CTRL} and cDC_{LPS} cultured alone and used as negative controls (Fig. 2C). These results revealed a higher chemoattractant capacity induced by the $pDC+cDC_{LPS}$ coculture. Blocking with an anti-CCL19 antibody confirmed that CCL19 was responsible, at least in part, for the increased migration observed (Fig. 2C).

Conditioned pDCs show a differential gene expression profile

The increased amount of CCL19 and IL-6 found in the coculture experiments was indicative of higher protein secretion by

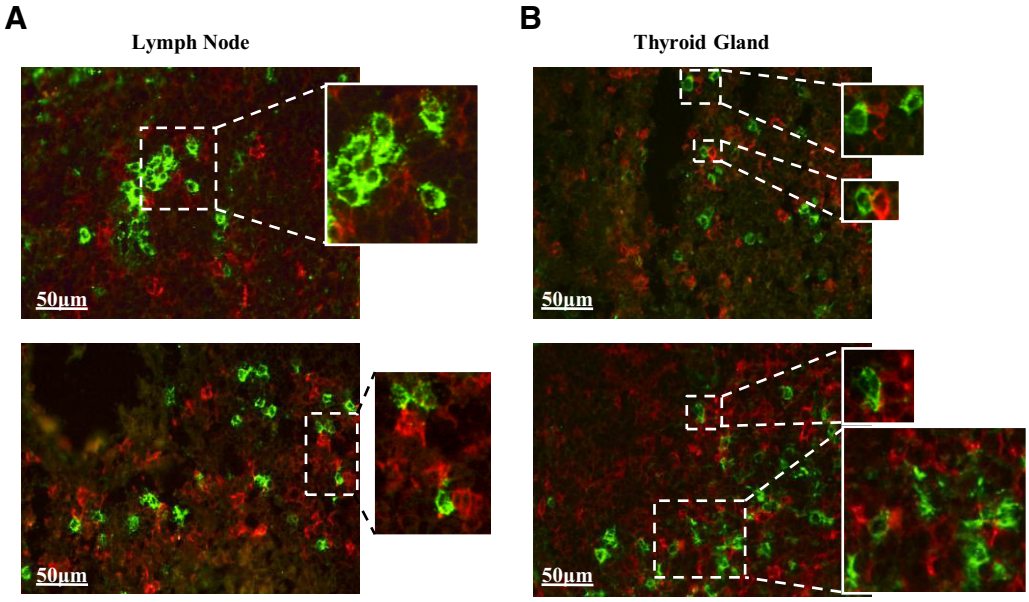

Figure 1. Human cDCs and pDCs are in close contact in healthy LNs and AITGs. Double immunofluorescence staining of 4 μm tissue cryosections is shown. pDCs (BDCA-2 in green) and cDCs (CD11c in red) are shown in different LNs (A) and AITD gland (B) sections. Original magnification, ×400; bars = 50 μm. Two different samples obtained from three LNs and six AITD glands examined are shown.

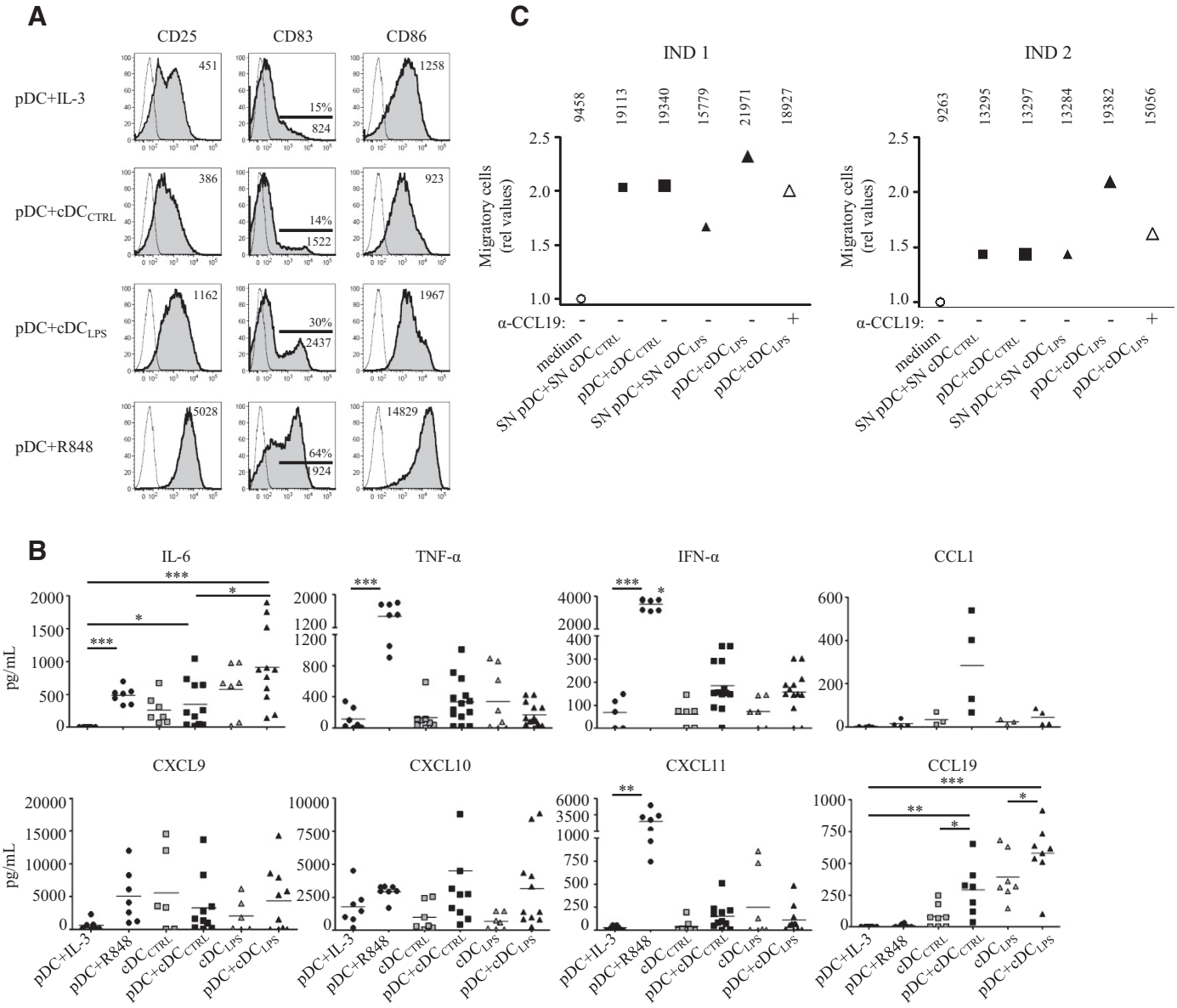

Figure 2. Coculture of pDCs+cDCs promotes phenotype changes on pDCs, higher IL-6 and CCL19 production, and CCL19 chemotaxis. Cells from each DC subset were sorted. pDCs were maintained in resting conditions and cDCs activated or not with LPS during 16 h. DC subsets were washed and cultured together at a 1:1 ratio during 24 h. (A) The expression of CD25, CD83, and CD86 (gray histograms) on pDCs cocultured with control (pDC+cDC$_{CTRL}$) or LPS-activated cDCs (pDC+cDC$_{LPS}$) was analyzed by flow cytometry. pDCs maintained in control conditions (pDC+IL-3) or activated with R848 (pDC+R848) are shown for comparative purposes. White histograms show the isotype controls. Numbers indicate the proportion of positive cells (%) or the mean fluorescence intensity (number) for each marker. A representative experiment of five is shown. (B) Sorted cDCs were stimulated or not for 16 h, washed and cultured in fresh medium, or cocultured with pDCs for 24 h. SNs were then harvested and analyzed for the presence of the indicated cytokines and chemokines using a Luminex assay. Each panel shows the levels of the indicated factor in the presence or absence of pDCs. As before, pDC+IL-3 and pDC+R848 are shown for comparison. Dots represent individual observations, and bars indicate the mean of at least seven independent experiments (*P<0.05; **P<0.01; ***P<0.001). (C) Sorted pDCs were maintained in IL-3, whereas sorted cDCs were activated or not during 16 h. After that period of time, cells were washed, counted, cultured and again separated, or cocultured. After 24 h, SNs of pDCs were mixed with SNs of cDC$_{CTRL}$ (SN pDC+SN cDC$_{CTRL}$) or cDC$_{LPS}$ (SN pDC+SN cDC$_{LPS}$; control SNs of cocultures). Combined SNs and SNs harvested from cocultures (pDC+cDC$_{CTRL}$; pDC+cDC$_{LPS}$), were incubated with antagonistic antibodies for CCL19 (α-CCL19: +) or with total human IgGs (α-CCL19: −) during 30 min, previous to their placing in the lower migration chamber. Autologous PBMCs (150×10^3) were disposed on the upper chamber. After 4 h at 37°C and 5% CO_2, 50 μl of the content of the lower chamber was harvested and used for counting total migratory cells. The results are normalized to the negative control condition containing only medium (basal migration=1). Numbers on the graph indicate total migratory cells counted. Results for two different individuals (IND 1 and IND 2) are shown.

cocultured DCs. To asess whether conditioned pDCs contributed to the pool of secreted cytokines/chemokines and to further investigate the mechanisms underlying the interaction between cDCs and pDCs, microarray analyses were performed on sorted pDCs following "conditioning" by cDCs. Coculture conditions were the same as before but were only maintained for 5 h to identify early modulated genes responding to the conditioning (**Fig. 3A**). At this time-point, $CFSE^{hi}CD11c^{-}$ pDCs were sorted and processed for mRNA extraction and analyses. The purity of these cells was demonstrated by the expression of CD123, BDCA-2, and HLA-DR (Fig. 3B). For the purpose of clarity, in the following results, $pDC_{[cDC\ CTRL]}$ will refer to sorted pDCs previously cocultured with control cDCs and $pDC_{[cDC\ LPS]}$, to sorted pDCs previously cocultured with LPS-activated cDCs.

Microarray results displayed 44 genes DE between $pDC_{[cDC\ LPS]}$ and their control condition $pDC_{[cDC\ CTRL]}$. For informative purposes, the pDC+IL-3 condition is also shown (Fig. 3C). These DE genes included up-regulated cytokines and chemokines, such as IL-6, IL-23A, CCL1, and CCL19. There were also regulators of cell survival (PIM2, BCL2L1), negative regulators of cell migration (ABI3, FGR), and transcription activator factors (BATF, BCL3, GATA3). Other important up-regulated, immune-related genes were the costimulatory molecule ICOS, the scavenger receptor SCARA5, and the negative regulatory molecule suppressor of cytokine signaling 3. In contrast, the chemokine receptor CCR2, which specifically mediates monocyte chemotaxis, was down-regulated. Interestingly, several Notch target and related genes, including HEY1, IL-7R, and NRARP, were up-regulated. Of note, none of the up-/down-

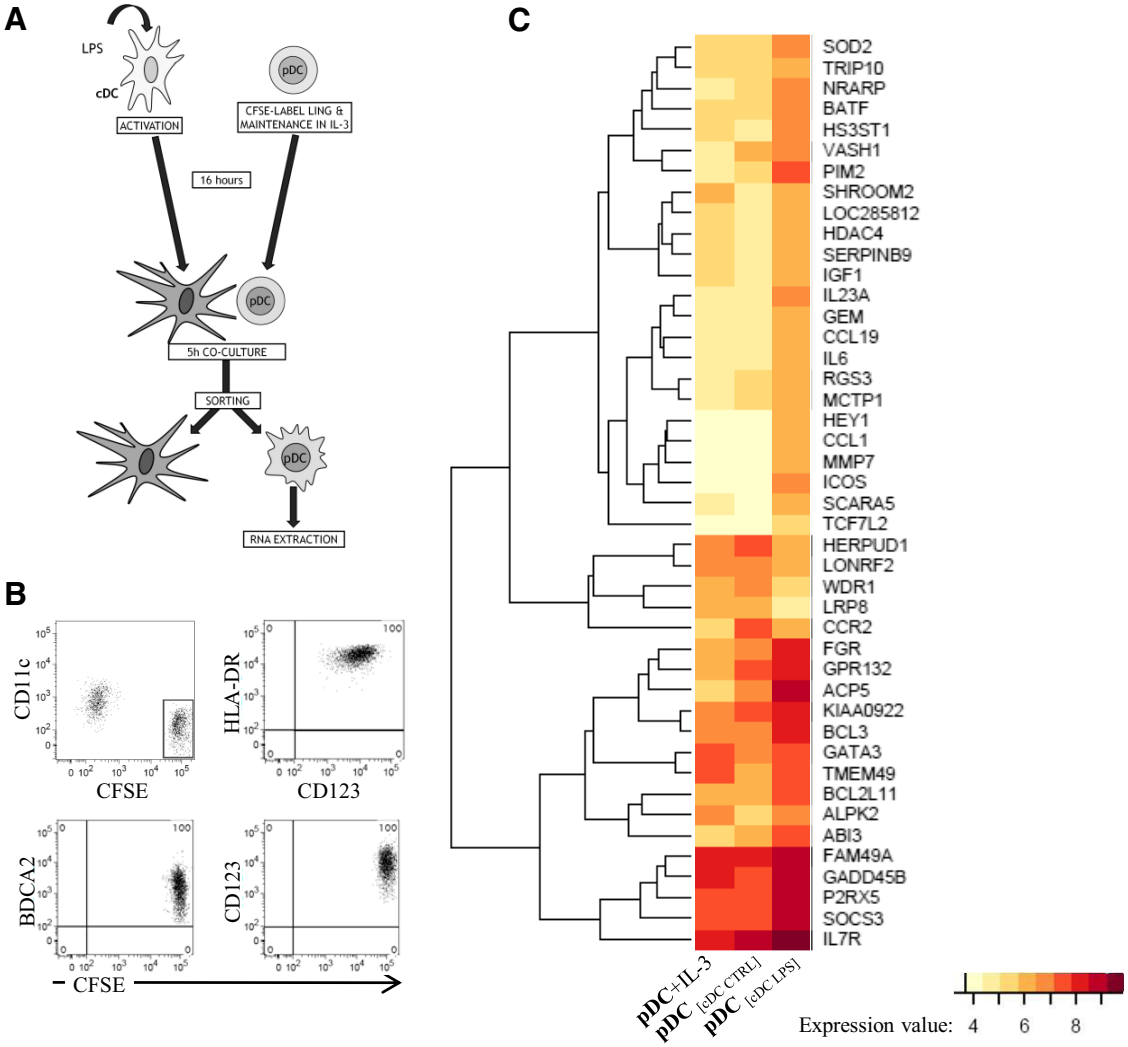

Figure 3. Conditioned pDCs show a differential gene expression profile. (A) Cells from each DC subset were sorted and cultured. pDCs were maintained in resting conditions and cDCs activated or not with LPS during 16 h. Then, cells were washed extensively and cultured together at a 1:1 ratio during 5 h. Then, pDCs were sorted again as CFSE+ CD11c−, and their RNA was extracted for gene expression studies. (B) The purity of these sorted, conditioned pDCs was confirmed by CD123, BDCA-2, and HLA-DR staining. A representative experiment of >30 sorting procedures is shown. (C) Heat map representing the expression values of all of the DE genes between $pDC_{[cDC\ CTRL]}$ and $pDC_{[cDC\ LPS]}$ as the median obtained in three independent experiments, ordered by hierarchical clustering. The pDC+IL-3 condition is shown for comparison. The legend indicates the equivalence between color code and expression values.

TABLE 1. Microarray Results for the Expression of Canonical Notch Target Genes on pDCs Conditioned by cDCs

Gene	pDC+IL-3	$pDC_{[cDC\ CTRL]}$	$pDC_{[cDC\ LPS]}$
HEY1	4.14	4.18	6.25[a]
IL-7R	8.46	8.55	9.92[b]
BATF	5.37	5.35	7.05[a]

Results are shown in median fluorescence intensity as the mean of three independent experiments. [a]$P < 0.001$; [b]$P < 0.05$.

modulated genes detected in our study was related to the IFN signature.

Conditioned pDCs undergo Notch activation

As mentioned, microarray data revealed an increased expression of some Notch target genes on $pDC_{[cDC\ LPS]}$ (**Table 1**). Recently, our group has characterized the presence and function of Notch receptors and ligands on human resting and activated cDCs and pDCs [27]. Furthermore, Notch signaling has been involved in the communication among immune cells (reviewed in ref. [28]). Thus, to validate the microarray results and also, to unravel the putative role of Notch in DC coordination, the expression of the canonical Notch target genes HEY1 and HES1 was analyzed by real-time RT-PCR. In these experiments, pDCs were maintained in control conditions (pDC+IL3) or cocultured with cDC_{CTRL} or cDC_{LPS} in the presence or absence of the specific γ-secretase inhibitor DAPT. Additional experiments were set up using $cDC_{P(I:C)}$ and the soluble Notch ligand Jag1 as a competitor for receptor-ligand interactions. $pDC_{[cDC\ CTRL]}$ and $pDC_{[cDC\ LPS]}$ showed significantly higher expression of the two Notch target genes compared with pDC+IL-3, thus clearly suggesting a Notch interaction. Further, in line with the microarray results, $pDC_{[cDC\ LPS]}$ showed an even higher expression of HEY1 compared with $pDC_{[cDC\ CTRL]}$. Addition of the γ-secretase inhibitor DAPT to the cocultures almost completely abrogated the induced gene expression. Similar results were observed in $pDC_{[cDC\ P(I:C)]}$ (**Fig. 4A**). Moreover, the soluble ligand Jag1 competed in all conditions tested with cell-expressed ligands preventing Notch-dependent interaction between DC subsets. This resulted in a significantly lower expression of HEY1 and HES1 in conditioned pDCs (Fig. 4B). Thus, these results clearly demonstrate that an activation of the Notch signaling pathway exists in pDCs conditioned by cDCs.

γ-Secretase activity is involved in CCL19 secretion by conditioned pDCs

Given the higher amounts of IL-6 and CCL19 found in SNs from pDCs+cDCs cocultures (Fig. 2B) and the increased expression of these genes in sorted pDCs conditioned by cDCs (Fig. 3C), we aimed to investigate whether Notch was involved in the induced expression of these molecules in conditioned pDCs. In fact, our group has previously reported the effects of DAPT on the production of CCL19 by pDCs and cDCs [27]. Thus, to study the involvement of Notch signaling between TLR-activated cDCs and pDCs on CCL19 production, a new set of experiments was performed. In line with the data obtained from the microarray analyses, $pDC_{[cDC\ LPS]}$ showed higher expression of IL-6 and CCL19 compared with $pDC_{[cDC\ CTRL]}$. The presence of DAPT in the cocultures hampered the up-regulation of CCL19 mRNA but not that of IL-6,

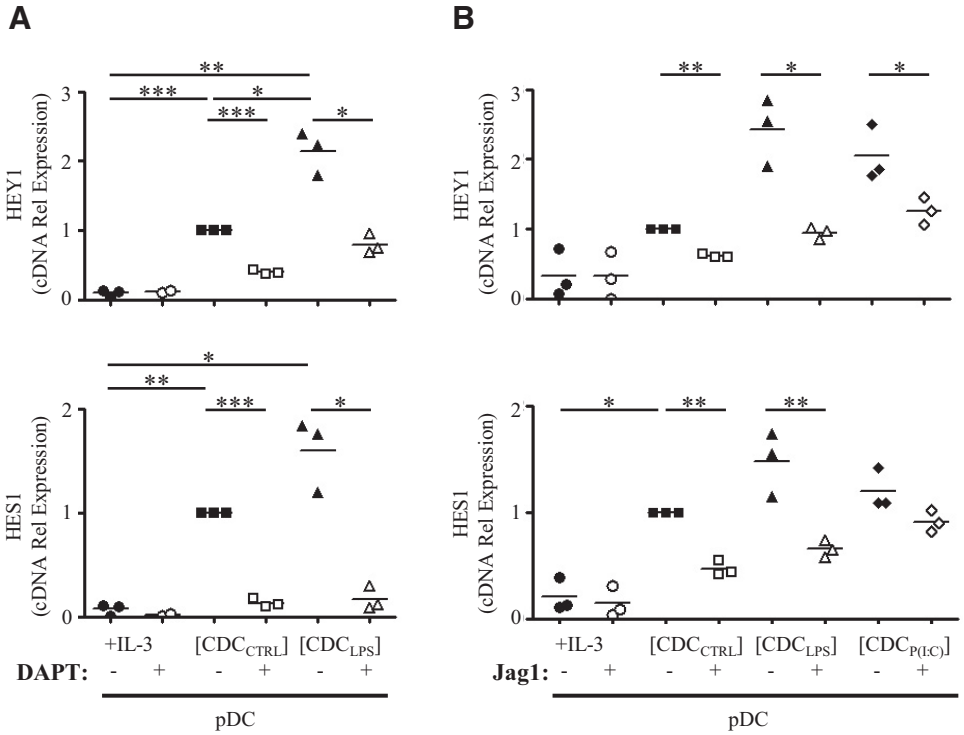

Figure 4. Notch signaling pathway is activated on conditioned pDCs. (A) IL-3-maintained pDCs were or not cocultured during 5 h with cDC_{CTRL} or cDC_{LPS} in the absence or presence of DAPT (−/+, black/white symbols). Then, pDCs were sorted, and the expression of the Notch target genes HES1 and HEY1 was analyzed by real-time RT-PCR. The results were normalized to the control condition $pDC_{[cDC\ CTRL]}$ (basal value=1). Each symbol represents an independent experiment. Bars indicate the mean of the three experiments performed (*P<0.05; **P<0.01; ***P<0.001). (B) IL-3-maintained pDCs were or not cocultured during 5 h with cDC_{CTRL}, cDC_{LPS}, or $cDC_{P(I:C)}$ in the absence or presence of sJag1 (−/+, black/white symbols). Then, pDCs were sorted, and the expression of the Notch target genes HES1 and HEY was analyzed by real-time RT-PCR. The results were normalized to the control condition $pDC_{[cDC\ CTRL]}$ (basal value=1). Each symbol represents an independent experiment. Bars indicate the mean of the three experiments performed (*P<0.05; **P<0.01).

revealing a possible regulatory role of Notch signaling in the regulation of CCL19 transcription on pDCs (**Fig. 5A**). These results were confirmed at the protein level, as the higher secretion of CCL19 detected on SNs from 24-h pDC+cDC_{LPS} cultures was diminished significantly in the presence of DAPT, whereas IL-6 secretion remained unchanged (Fig. 5B). Although a direct effect of DAPT on cDCs may also be considered, the RT-PCR results confirmed that pDCs were unequivocally producing this cytokine. Confirming the observation made on $pDC_{[cDC\ LPS]}$, $pDC_{[cDC\ P(I:C)]}$ also showed increased IL-6 and CCL19 gene expression (Figs. 5C). We then used the soluble Notch ligand Jag1 as a competitor for the cellular Notch receptor-ligand signaling events. In these conditions, the increased expression of CCL19 could not be abrogated (Fig. 5C), as it happened for the canonical Notch target genes. Therefore, CCL19 overexpression on conditioned pDCs is dependent on a γ-secretase mechanism rather than the Notch pathway.

DISCUSSION

Mounting a rapid and effective immune response requires the participation of multiple cell types, from APCs to effector lymphocytes. As a result of their intrinsic capacity to respond to a specific stimulus and their different migratory behavior, DC subsets will preferentially act as the "leaders" during antigen presentation or as the "followers". These followers will provide additional help, which may be crucial in certain conditions. For instance, in the context of bacterial infections, in which pDCs would faintly respond, these cells may play an accessory role. This DC intercommunication might also be important to increase sensitivity to less-potent or limited stimuli [14], a situation which may well occur during antigen sampling and transport by cDCs, as described in intranasal-administered latex particles [29], or in the early stages of pathogen infection. It may also contribute to maintain higher levels of cytokine or chemokine secretion after the initial burst produced by cDCs

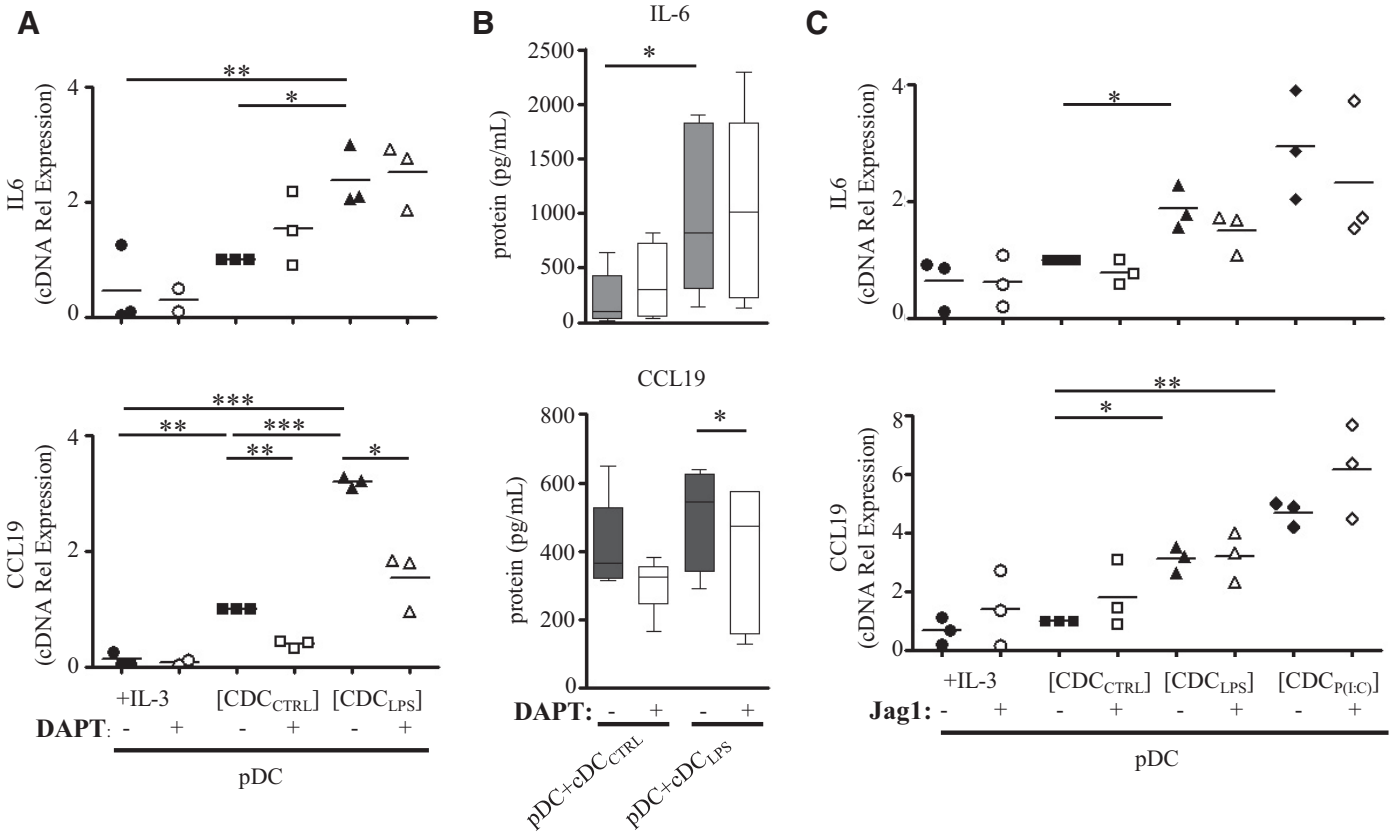

Figure 5. γ-Secretase complex, but not Notch signaling pathway, regulates CCL19 expression. (A) IL-3-maintained pDCs were or not cocultured during 5 h with cDC_{CTRL} or cDC_{LPS} in the absence or presence of DAPT (−/+, black/white symbols). Then, pDCs were sorted, and the expression of IL-6 and CCL19 was analyzed by real-time RT-PCR. Results were normalized to control condition $pDC_{[cDC\ CTRL]}$ (basal value=1). Each symbol represents an independent experiment. Bars indicate the mean of three experiments (*P<0.05; **P<0.01; ***P<0.001). (B) Sorted cDCs were or not LPS-stimulated during 16 h, washed, and cocultured with pDCs during an additional 24 h in the presence (+, white boxes) or absence (−, gray boxes) of DAPT. SNs were then harvested and analyzed for the presence of IL-6 and CCL19 using a Luminex assay. Box plots indicate the median (line) and percentiles of five independent experiments (*P<0.05). (C) IL-3-maintained pDCs were or not cocultured during 5 h with cDC_{CTRL}, cDC_{LPS}, or $cDC_{P(I:C)}$ in the absence or presence of sJag1 (−/+, black/white symbols). Then, pDCs were sorted, and the expression of IL-6 and CCL19 was analyzed by real-time RT-PCR. Results were normalized to control condition $pDC_{[cDC\ CTRL]}$ (basal value=1). Each symbol represents an independent experiment. Bars indicate the mean of three experiments (*P<0.05; **P<0.01).

and other cells at the site of inflammation. Thus, coordination between DC subsets may represent an advantage to induce a potent immune response. In this sense, coordination between DC populations has been suggested by several reports in mice [15–17, 30] and humans [13, 14, 31]. Importantly, this coordination is dependent on cell contact events. In fact, here, we show that cells from each DC subset may be found in close contact in human LNs and in infiltrating autoimmune thyroid tissue. These contacts had been also reported in the skin of cutaneous lupus erythematosus patients [11] and in human spleen [12]. These data support that cell contacts between both DC subsets occur in vivo.

In mice, LN-recruited pDCs help cDCs to improve CTL induction through CD2-CD2L and CD40L-CD40 interactions [15]. Similarly, coordinate effects of murine pDCs on cDCs have been reported to be dependent on CD40-CD40L interactions, together with IL-15 secretion [16], whereas in humans and pigs, IFN-α played a crucial role [18–20, 32]. Cell contact is also essential for DC cross-talk in humans [13], but CD40 blockade has no effect on the reciprocal maturation between cDCs and pDCs [14], suggesting that other mechanisms and factors are involved. Using circulating human DCs and a microarray approach, here, we show that TLR-activated cDCs may induce maturation and functional activity of pDCs through mechanisms involving the catabolic enzyme γ-secretase, including the Notch signaling pathway.

Previous studies demonstrated an enhanced antigen-presenting capacity of pDCs and cDCs as a result of DC cross-talk, as indicated by an increased expression of maturation markers and an alloproliferative response [13, 14]. Similarly, our data confirm the induction of an activated phenotype on conditioned pDCs. Of special interest is the increase of CD25 (a well-known Notch target gene) on $pDC_{[cDC\ LPS]}$, which may facilitate the delivery of IL-2 to T cells, thus helping in T cell expansion and antigen-specific effector development [33]. Moreover, we detected higher amounts of IL-6 and CCL19, which promoted a higher rate of cell migration, in SNs of cocultured $pDC+cDC_{LPS}$. Unfortunately, intracellular staining did not allow the unequivocal identification of the CCL19-producing subset in the coculture experiments (data not shown). However, gene expression analyses revealed higher expression of IL-6 and CCL19 mRNA in sorted $pDC_{[cDC\ CTRL]}$ and especially, in $pDC_{[cDC\ LPS]}$ and $pDC_{[cDC\ P(I:C)]}$ compared with pDC+IL-3. This indicates that conditioned pDCs are, at least in part, responsible for the increased cytokine/chemokine secretion detected in SNs. Thus, our results further confirm the conditioning of pDCs by TLR-activated cDCs. Several authors consider that pDCs use their MHC-II antigen-presentation machinery in a manner that is qualitatively distinct to cDCs, and they argue for a complementary role between cDCs and pDCs during antigen presentation to $CD4^+$ T cells [34, 35]. Wolf et al. [36] suggested that pDCs regulate the accumulation of T cells in the bronchoalveolar space during early influenza virus infection. Recently it has been shown that pDCs are required during the inflammation triggered by TLR ligands and by viral or bacterial infections. In these contexts, their role is to control effector and regulatory $CD4^+$ T cell homeostasis and to initiate $CD8^+$ T cell responses [37]. CCL19 mediates attracting $CCR7^+$ cells, which mainly correspond to naive and central memory T cells [38]. Our results demonstrate that increased levels of CCL19 induce cell migration, and thus, coordination between DC subsets may participate in T cell recruitment and activation of this cell type.

Interestingly, from the microarray analyses in sorted pDCs, the increase in the negative regulators of cell migration ABI3 and FGR [39–41] may help to retain pDCs at sites of antigen presentation. These changes may contribute to a putative accessory function of pDCs. Accordingly, no evidences of IFN-α signaling activation were detected on sorted, conditioned pDCs. Furthermore, a negative regulator of IFN-α production, ACP5 [42], was up-regulated in $pDC_{[cDC\ LPS]}$. These results are in agreement with recent published data showing that TLR2- or TLR4-activated monocytes inhibit IFN-α production by pDCs, ensuring that the IFN-α response is only induced in the presence of viral infection, together with the absence of bacterial infection [31]. Therefore, communication from LPS-activated cDCs to pDCs would guarantee the generation of the required pathogen-specific immune response (bacterial vs. viral).

So far, coordination between human DCs has been shown to depend on cell contact, but the molecules involved in such coordination have not been identified. Here, data obtained from gene expression analyses revealed the putative involvement of the Notch signaling pathway in the human cDC/pDC cross-talk, as already observed in other immune cells. The Notch signaling pathway is a well-conserved cell contact-dependent mechanism involved in an extensive number of cellular functions. Notch signaling has an important role in defining Th cell polarization in mice and humans (reviewed in ref. [28]) and in the cytotoxic activity of NK cells induced by DCs [43]. Regarding DCs, Notch ligation has been demonstrated to induce maturation on human monocyte-derived DCs [44] and mice bone marrow-derived DCs [45]. Recently, our group has described the expression and function of Notch receptors and ligands on human DC subsets [27]. In line with our previous study, the γ-secretase inhibitor DAPT blocked the induction of maturation markers, such as CD83 on pDCs (data not shown), and hampered CCL19 production in pDCs+cDCs cocultures. However, competition experiments using sJag1 significantly restrained the expression of Notch target genes but not of CCL19. Therefore, additional mechanisms unequivocally dependent on the γ-secretase dictate the fate of conditioned pDCs in coculture experiments. The γ-secretase enzymatic complex cleaves single-pass transmembrane proteins at residues within the transmembrane domain. A sequential processing of the transmembrane chemokines CX3CL1 and CXCL16 by α- and γ-secretases has been reported [46]. As CCL19 is considered a nontransmembrane chemokine, the involvement of DAPT in CCL19 secretion is unknown. The induction of CCL19 (and other genes), not related to the Notch signaling pathway, points toward additional signaling events between cDCs and pDCs to promote pDC conditioning. Beyond this observation, the Notch pathway is clearly activated in the receptor-ligand interaction between pDCs and cDCs, but the final consequences of this interaction require further investigation.

In summary, to our best knowledge, this is the first study to show gene and protein activation on conditioned pDCs promoted by TLR-activated cDCs. Importantly, our results also provide strong evidence for the involvement of Notch receptor-ligand interactions in this communication, suggesting the Notch signaling pathway as one of the mechanisms involved in human DC cooperation. This coordination between cDCs and pDCs may in turn contribute to establish a specific immunostimulatory environment, further supporting the view that a cooperative relationship between human DC subsets may be important in the induction of the specialized immune response to a given danger signal.

AUTHORSHIP

B.P-C. performed the experiments, analyzed data, made the figures, and wrote the manuscript; M.N-G. and P.B-A. performed some experiments and revised the manuscript; M.R-R. performed and analyzed the immunofluorescence staining of tissue sections; M.A.F. performed flow cytometry cell sorting; F.C. directed statistical analyses of microarray data; F.N. directed microarray experiments; R.P-B. analyzed data and revised the manuscript; F.E.B. designed and conducted the study, organized the data, and wrote the paper.

ACKNOWLEDGMENTS

This work has been supported by a grant from the "Fondo de Investigaciones Sanitarias" of the Spanish National Institute of Health (FIS 06/0453) to F.E.B.. B.P-C. is supported by a grant from the Instituto de Salud Carlos III of the Spanish National Institute of Health (FI07/00054). M.N-G. is supported by a grant from the Spanish Ministry of Science and Innovation and Blood and Tissue Bank (PTQ-09-02-017050). F.E.B. is cofunded by the stabilization program of biomedical researchers (CES 07/015) of the Instituto de Salud Carlos III and Direcció d'Estratègia i Coordinació, Health Department of the Catalan government. The authors thank the Catalan BST for the continuous support. We also thank Drs. Daniel Benítez-Ribas and María Montoya (of the Catalan group for the study of DCs, DC-CAT) for suggestions and for critically reviewing the manuscript.

REFERENCES

1. Robinson, S. P., Patterson, S., English, N., Davies, D., Knight, S. C., Reid, C. D. (1999) Human peripheral blood contains two distinct lineages of dendritic cells. *Eur. J. Immunol.* **29,** 2769–2778.
2. Dzionek, A., Fuchs, A., Schmidt, P., Cremer, S., Zysk, M., Miltenyi, S., Buck, D. W., Schmitz, J. (2000) BDCA-2, BDCA-3, and BDCA-4: three markers for distinct subsets of dendritic cells in human peripheral blood. *J. Immunol.* **165,** 6037–6046.
3. Borràs, F. E., Matthews, N. C., Lowdell, M. W., Navarrete, C. V. (2001) Identification of both myeloid CD11c+ and lymphoid CD11c− dendritic cell subsets in cord blood. *Br. J. Haematol.* **113,** 925–931.
4. Banchereau, J., Briere, F., Caux, C., Davoust, J., Lebecque, S., Liu, Y. J., Pulendran, B., Palucka, K. (2000) Immunobiology of dendritic cells. *Annu. Rev. Immunol.* **18,** 767–811.
5. Shortman, K., Liu, Y. J. (2002) Mouse and human dendritic cell subtypes. *Nat. Rev. Immunol.* **2,** 151–161.
6. Young, L. J., Wilson, N. S., Schnorrer, P., Proietto, A., ten Broeke, T., Matsuki, Y., Mount, A. M., Belz, G. T., O'Keeffe, M., Ohmura-Hoshino, M., Ishido, S., Stoorvogel, W. W. R. Heath, Shortman, K., Villadangos, J. A. (2008) Differential MHC class II synthesis and ubiquitination confers distinct antigen-presenting properties on conventional and plasmacytoid dendritic cells. *Nat. Immunol.* **9,** 1244–1252.
7. Dalgaard, J., Beckstrøm, K. J., Jahnsen, F. L., Brinchmann, J. E. (2005) Differential capability for phagocytosis of apoptotic and necrotic leukemia cells by human peripheral blood dendritic cell subsets. *J. Leukoc. Biol.* **77,** 689–698.
8. Andersson, L. I., Hellman, P., Eriksson, H. (2008) Receptor-mediated endocytosis of particles by peripheral dendritic cells. *Hum. Immunol.* **69,** 625–633.
9. Sadaka, C., Marloie-Provost, M. A., Soumelis, V., Benaroch, P. (2009) Developmental regulation of MHC II expression and transport in human plasmacytoid-derived dendritic cells. *Blood* **113,** 2127–2135.
10. Bastos-Amador, P., Pérez-Cabezas, B., Izquierdo-Useros, N., Puertas, M. C., Martinez-Picado, J., Pujol-Borell, R., Naranjo-Gómez, M., Borras, F. E. (2012) Capture of cell-derived microvesicles (exosomes and apoptotic bodies) by human plasmacytoid dendritic cells. *J. Leukoc. Biol.*, Epub ahead of print.
11. Vermi, W., Lonardi, S., Morassi, M., Rossini, C., Tardanico, R., Venturini, M., Sala, R., Tincani, A., Poliani, P. L., Calzavara-Pinton, P. G., Cerroni, L., Santoro, A., Facchetti, F. (2009) Cutaneous distribution of plasmacytoid dendritic cells in lupus erythematosus. Selective tropism at the site of epithelial apoptotic damage. *Immunobiology* **214,** 877–886.
12. Nascimbeni, M., Peri, L. é, Chorro, L., Diocou, S., Kreitmann, L., Louis, S., Garderet, L., Fabiani, B., Berger, A., Schmitz, J., Marie, J. P., Molina, T. J., Pacanowski, J., Viard, J. P., Oksenhendler, E., Beq, S., Abehsira-Amar, O., Cheynier, R., Hosmalin, A. (2009) Plasmacytoid dendritic cells accumulate in spleens from chronically HIV-infected patients but barely participate in interferon-α expression. *Blood* **113,** 6112–6119.
13. Naranjo-Gómez, M., Fernández, M. A., Bofill, M., Singh, R., Navarrete, C. V., Pujol-Borrell, R., Borràs, F. E. (2005) Primary alloproliferative TH1 response induced by immature plasmacytoid dendritic cells in collaboration with myeloid DCs. *Am. J. Transplant.* **5,** 2838–2848.
14. Piccioli, D., Sammicheli, C., Tavarini, S., Nuti, S., Frigimelica, E., Manetti, A. G., Nuccitelli, A., Aprea, S., Valentini, S., Borgogni, E., Wack, A., Valiante, N. M. (2009) Human plasmacytoid dendritic cells are unresponsive to bacterial stimulation and require a novel type of cooperation with myeloid dendritic cells for maturation. *Blood* **113,** 4232–4239.
15. Yoneyama, H., Matsuno, K., Toda, E., Nishiwaki, T., Matsuo, N., Nakano, A., Narumi, S., Lu, B., Gerard, C., Ishikawa, S., Matsushima, K. (2005) Plasmacytoid DCs help lymph node DCs to induce anti-HSV CTLs. *J. Exp. Med.* **202,** 425–435.
16. Kuwajima, S., Sato, T., Ishida, K., Tada, H., Tezuka, H., Ohteki, T. (2006) Interleukin 15-dependent crosstalk between conventional and plasmacytoid dendritic cells is essential for CpG-induced immune activation. *Nat. Immunol.* **7,** 740–746.
17. Lou, Y., Liu, C., Kim, G. J., Liu, Y. J., Hwu, P., Wang, G. (2007) Plasmacytoid dendritic cells synergize with myeloid dendritic cells in the induction of antigen-specific antitumor immune responses. *J. Immunol.* **178,** 1534–1541.
18. Fonteneau, J. F., Larsson, M., Beignon, A. S., McKenna, K., Dasilva, I., Amara, A., Liu, Y. J., Lifson, J. D., Littman, D. R., Bhardwaj, N. (2004) Human immunodeficiency virus type 1 activates plasmacytoid dendritic cells and concomitantly induces the bystander maturation of myeloid dendritic cells. *J. Virol.* **78,** 5223–5232.
19. Megjugorac, N. J., Jacobs, E. S., Izaguirre, A. G., George, T. C., Gupta, G., Fitzgerald-Bocarsly, P. (2007) Image-based study of interferongenic interactions between plasmacytoid dendritic cells and HSV-infected monocyte-derived dendritic cells. *Immunol. Invest.* **36,** 739–761.
20. Chen, W., Zhang, Z., Shi, M., Chen, L., Fu, J., Shi, F., Zhang, B., Zhang, H., Jin, L., Wang, F. S. (2008) Activated plasmacytoid dendritic cells act synergistically with hepatitis B core antigen-pulsed monocyte-derived dendritic cells in the induction of hepatitis B virus-specific CD8 T-cell response. *Clin. Immunol.* **129,** 295–303.
21. Morohashi, Y., Kan, T., Tominari, Y., Fuwa, H., Okamura, Y., Watanabe, N., Sato, C., Natsugari, H., Fukuyama, T., Iwatsubo, T., Tomita, T. (2006) C-terminal fragment of presenilin is the molecular target of a dipeptidic γ-secretase-specific inhibitor DAPT (N-[N-(3,5-difluorophenacetyl)-L-alanyl]-S-phenylglycine t-butyl ester). *J. Biol. Chem.* **281,** 14670–14676.
22. Ruiz-Riol, M., Barnils Mdel, P., Colobran, Oriol, R., Pla, A. S., Borràs Serres, F. E., Lucas-Martin, A., Cáceres, E. M., Pujol-Borrell, R. (2011) Analysis of the cumulative changes in Graves' disease thyroid glands points to IFN signature, plasmacytoid DCs and alternatively activated macrophages as chronicity determining factors. *J. Autoimmun.* **36,** 189–200.
23. Armengol, M. P., Juan, M., Lucas-Martín, A., Fernández-Figueras, M. T., Jaraquemada, D., Gallart, T., Pujol-Borrell, R. (2001) Thyroid autoimmune disease: demonstration of thyroid antigen-specific B cells and recombination-activating gene expression in chemokine-containing active intrathyroidal germinal centers. *Am. J. Pathol.* **159,** 861–873.
24. Smyth, G. K. (2004) Linear models and empirical bayes methods for assessing differential expression in microarray experiments. *Stat. Appl. Genet. Mol. Biol.* **3,** Article3.
25. Gentleman, R. C., Carey, V. J., Bates, D. M., Bolstad, B., Dettling, M., Dudoit, S., Ellis, B., Gautier, L., Ge, Y., Gentry, J., Hornik, K., Hothorn,

T., Huber, W., Iacus, S., Irizarry, R., Leisch, F., Li, C., Maechler, M., Rossini, A. J., Sawitzki, G., Smith, C., Smyth, G., Tierney, L., Yang, J. Y., Zhang, J. (2004) Bioconductor: open software development for computational biology and bioinformatics. *Genome Biol.* **5,** R80.
26. O'Garra, A., Vieira, P. (1992) Polymerase chain reaction for detection of cytokine gene expression. *Curr. Opin. Immunol.* **4,** 211–215.
27. Pérez-Cabezas, B., Naranjo-Gómez, M., Bastos-Amador, P., Requena-Fernández, G., Pujol-Borrell, R., Borràs, F. E. (2011) Ligation of Notch receptors in human conventional and plasmacytoid dendritic cells differentially regulates cytokine and chemokine secretion and modulates Th cell polarization. *J. Immunol.* **186,** 7006–7015.
28. Cheng, P., Zhou, J., Gabrilovich, D. (2010) Regulation of dendritic cell differentiation and function by Notch and Wnt pathways. *Immunol. Rev.* **234,** 105–119.
29. Jakubzick, C., Tacke, F., Llodra, J., van Rooijen, N., Randolph, G. J. (2006) Modulation of dendritic cell trafficking to and from the airways. *J. Immunol.* **176,** 3578–3584.
30. Allan, R. S., Waithman, J., Bedoui, S., Jones, C. M., Villadangos, J. A., Zhan, Y., Lew, A. M., Shortman, K., Heath, W. R., Carbone, F. R. (2006) Migratory dendritic cells transfer antigen to a lymph node-resident dendritic cell population for efficient CTL priming. *Immunity* **25,** 153–162.
31. Poth, J. M., Coch, C., Busch, N., Boehm, O., Schlee, M., Janke, M., Zillinger, T., Schildgen, O., Barchet, W., Hartmann, G. (2010) Monocyte-mediated inhibition of TLR9-dependent IFN-α induction in plasmacytoid dendritic cells questions bacterial DNA as the active ingredient of bacterial lysates. *J. Immunol.* **185,** 7367–7373.
32. Kramer, M., Schulte, B., Eleveld-Trancikova, M., van Hout-Kuijer, D. M., Toonen, L. W., Tel, J., de Vries, I. J., van Kuppeveld, F. J., Jansen, B. J., Adema, G. J. (2010) Cross-talk between human dendritic cell subsets influences expression of RNA sensors and inhibits picornavirus infection. *J. Innate Immun.* **2,** 360–370.
33. Wuest, S. C., Edwan, J. H., Martin, J. F., Han, S., Perry, J. S., Cartagena, C. M., Matsuura, E., Maric, D., Waldmann, T. A., Bielekova, B. (2011) A role for interleukin-2 trans-presentation in dendritic cell-mediated T cell activation in humans, as revealed by daclizumab therapy. *Nat. Med.* **5,** 604–609.
34. Randolph, G. J., Ochando, J., Partida-Sánchez, S. (2008) Migration of dendritic cell subsets and their precursors. *Annu. Rev. Immunol.* **26,** 293–316.
35. Segura, E., Villadangos, J. A. (2009) Antigen presentation by dendritic cells in vivo. *Curr. Opin. Immunol.* **21,** 105–110.
36. Wolf, A. I., Buehler, D., Hensley, S. E., Cavanagh, L. L., Wherry, E. J., Kastner, P., Chan, S., Weninger, W. (2009) Plasmacytoid dendritic cells are dispensable during primary influenza virus infection. *J. Immunol.* **182,** 871–879.
37. Takagi, H., Fukaya, T., Eizumi, K., Sato, Y., Sato, K., Shibazaki, A., Otsuka, H., Hijikata, A., Watanabe, T., Ohara, O., Kaisho, T., Malissen, B., Sato, K. (2011) Plasmacytoid dendritic cells are crucial for the initiation of inflammation and T cell immunity in vivo. *Immunity* **6,** 958–971.
38. Ebert, L. M., Schaerli, P., Moser, B. (2005) Chemokine-mediated control of T cell traffic in lymphoid and peripheral tissues. *Mol. Immunol.* **42,** 799–809.
39. Zhang, Z., Andoh, A., Yasui, H., Inatomi, O., Hata, K., Tsujikawa, T., Kitoh, K., Takayanagi, A., Shimizu, N., Fujiyama, Y. (2005) Interleukin-1β and tumor necrosis factor-α upregulate interleukin-23 subunit p19 gene expression in human colonic subepithelial myofibroblasts. *Int. J. Mol. Med.* **15,** 79–83.
40. Latini, F. R., Hemerly, J. P., Oler, G., Riggins, G. J., Cerutti, J. M. (2008) Re-expression of ABI3-binding protein suppresses thyroid tumor growth by promoting senescence and inhibiting invasion. *Endocr. Relat. Cancer* **15,** 787–799.
41. Baruzzi, A., Iacobucci, I., Soverini, S., Lowell, C. A., Martinelli, G., Berton, G. (2010) c-Abl and Src-family kinases cross-talk in regulation of myeloid cell migration. *FEBS Lett.* **584,** 15–21.
42. Briggs, T. A., Rice, G. I., Daly, S., Urquhart, J., Gornall, H., Bader-Meunier, B., Baskar, K., Baskar, S., Baudouin, V., Beresford, M. W., Black, G. C., Dearman, R. J., de Zegher, F., Foster, E. S., Francès, C., Hayman, A. R., Hilton, E., Job-Deslandre, C., Kulkarni, M. L., Le, Merrer, M., Linglart, A., Lovell, S. C., Maurer, K., Musset, L., Navarro, V., Picard, C., Puel, A., Rieux-Laucat, F., Roifman, C. M., Scholl-Bürgi, S., Smith, N., Szynkiewicz, M., Wiedeman, A., Wouters, C., Zeef, L. A., Casanova, J. L., Elkon, K. B., Janckila, A., Lebon, P., Crow, Y. J. (2011) Tartrate-resistant acid phosphatase deficiency causes a bone dysplasia with autoimmunity and a type I interferon expression signature. *Nat. Genet.* **43,** 127–131.
43. Kijima, M., Yamaguchi, T., Ishifune, C., Maekawa, Y., Koyanagi, A., Yagita, H., Chiba, S., Kishihara, K., Shimada, M., Yasutomo, K. (2008) Dendritic cell-mediated NK cell activation is controlled by Jagged2-Notch interaction. *Proc. Natl. Acad. Sci. USA* **105,** 7010–7015.
44. Weijzen, S., Velders, M. P., Elmishad, A. G., Bacon, P. E., Panella, J. R., Nickoloff, B. J., Miele, L., Kast, W. M. (2002) The Notch ligand Jagged-1 is able to induce maturation of monocyte-derived human dendritic cells. *J. Immunol.* **169,** 4273–4278.
45. Bugeon, L., Gardner, L. M., Rose, A., Gentle, M., Dallman, M. J. (2008) Cutting edge: Notch signaling induces a distinct cytokine profile in dendritic cells that supports T cell-mediated regulation and IL-2-dependent IL-17 production. *J. Immunol.* **181,** 8189–8193.
46. Schulte, A., Schulz, B., Andrzejewski, M. G., Hundhausen, C., Mletzko, S., Achilles, J., Reiss, K., Paliga, K., Weber, C., John, S. R., Ludwig, A. (2007) Sequential processing of the transmembrane chemokines CX3CL1 and CXCL16 by α- and γ-secretases. *Biochem. Biophys. Res. Commun.* **1,** 233–240.

KEY WORDS:
human · dendritic cells · cooperation · Notch · CCL19 · γ-secretase